Estimation of Canopy Height Using an Airborne *Ku*-Band Frequency-Modulated Continuous Waveform Profiling Radar

Hui Zhou, Yuwei Chen, Juha Hyyppä, Ziyi Feng, Fashuai Li, Teemu Hakala, Xinmin Xu, and Xiaolei Zhu

***Abstract*—An airborne *Ku*-band frequency-modulated continuous waveform (FMCW) profiling radar terms as Tomoradar provides a distance-resolved measure of microwave radiation backscattered from the canopy surface and the underlying ground. The Tomoradar waveform data are acquired in the southern Boreal Forest Zone with Scots pine, Norway spruce, and birch as major species in Finland. A weighted filtering algorithm based on statistical properties of noise is designed to process the original waveform. In addition, another algorithm of estimating canopy height for the processed waveform is developed by extracting the canopy top and ground position. A higher-precision reference data from a Velodyne VLP-16 laser scanner and a digital terrain model are introduced to validate the accuracy of extracted canopy height. According to the processed results from 127 765 copolarization measurements in 32 stripes of Tomoradar field test, the mean error of canopy height varies from −0.04 to 1.53 m, and the root-mean-square error approximates 1 m. Moreover, the estimated canopy heights highly correlate with the reference data in view of that the correlation coefficients maintain from 0.86 to 0.99 with an average value of 0.96. All these results demonstrate that Tomoradar presents an important approach in estimating the canopy height with several meters footprint and is feasible of being a validation instrument for satellite LiDAR with large footprint in the forest inventory.**

***Index Terms*—Canopy height, *Ku* band profile radar, waveform, weighted filtering.**

Manuscript received November 24, 2017; revised July 6, 2018; accepted July 27, 2018. Date of publication September 12, 2018; date of current version October 15, 2018. This work was supported in part by the Academy of Finland project Interaction of Lidar/Radar Beams with Forests Using Mini-UAV and Mobile Forest Tomography and Centre of Excellence in Laser Scanning Research (CoE-LaSR) (272195), in part by the European Community's Seventh Framework Programmer (FP7/2007–2013) under Grant 606971, in part by the Chinese Academy of Science (181811KYSB20160113), in part by the Chinese Ministry of Science and Technology (2015DFA70930), and in part by the Shanghai Science and Technology Foundations (18590712600). *(Corresponding author: Yuwei Chen.)*

H. Zhou is with the Electronic Information School, Wuhan University, Wuhan 430072, China, and also with the Department of Remote Sensing and Photogrammetry, Finnish Geospatial Research Institute, Masala 02430, Finland (e-mail: zhouhui@whu.edu.cn).

Y. Chen, J. Hyyppä, Z. Feng, F. Li, and T. Hakala are with the Department of Remote Sensing and Photogrammetry, Finnish Geospatial Research Institute, Masala 02430, Finland (e-mail: yuwei.chen@nls.fi; juha.hyyppa@nls.fi; ziyi.feng@nls.fi; f.li@utwente.nl; teemu.hakala@nls.fi).

X. Xu and X. Zhu are with the College of Information Science and Electronic Engineering, Zhejiang University, Hangzhou 310027, China (e-mail: xuxm@zju.edu.cn; zhuxl@vlsi.zju.edu.cn).

Color versions of one or more of the figures in this paper are available online at http://ieeexplore.ieee.org.

Digital Object Identifier 10.1109/JSTARS.2018.2865624

I. Introduction

FORESTS are the dominant terrestrial ecosystem of Earth. It covers 30 percent of global land area, and distributes across the globe from the tropics or subtropics to the temperate zones and the coniferous boreal forests. Significant ecological processes, particularly the carbon cycle, are expressed in and are affected by the vertical structure of forest canopies. Thus, as a common used forest inventory parameter, canopy height plays a crucial role in the assessment of ecological variations among tree species, forest productivity, and standing growth rate. With the development of modern technologies, many remote sensing instruments including optical sensors, synthetic aperture radars (SAR), light detection and radar (LiDARs), microwave radars are employed to measure canopy height [1]–[5].

The electromagnetic wavelength and energy employed in the remote sensing apparatus physically determine the penetration property and the strength of received signal backscattering from the surface of vegetation. Passive airborne or spaceborne optical cameras mainly receive the reflected sunlight from the exterior canopy surface and have difficulties in acquiring the information under the canopy surface due to topographical occlusion, the limitation of employed spectral range, and bad weather condition. Therefore, they can hardly capture vertical forest structure directly and exclusively obtain the forest attributes such as tree crown and leaf area index [6]–[8]. Active LiDAR collects the reflected laser pulse signal mainly from the canopy surface, while a small part of which come from the ground surface [9]. However, LiDAR sensors normally utilize laser sources whose spectrum ranges from visible to infrared, thus it confronts a low penetration problem for vegetation with denser tree leaves. Therefore, the fusion approach of optical images and LiDAR data has been adopted in the retrieval of forest attributes [10], [11].

Compared with LiDAR sensors, active microwave sensors can collect data with longer wavelengths. Thereby they begin to play an increasingly important role in remote sensing of earth surfaces. It provides novel ways to understand environmental and earth system dynamics at local and global scales. Various spaceborne imaging radars, scatterometers, microwave altimeters, and SARs have been well developed in the past decades worldwide and operate on a wide frequency ranging from P-band to *Ka*-band, even VHF band [12]. They can capture information of ground properties due to their ability of detecting the

dielectric properties remotely. All these sensors have a unique feature that they can be operated for observation in a ubiquitously manner: the measurement is independent of illustration and usually is not sensitive to weather condition or cloud cover, which are major restrictions of optical sensors. Thus, they are particularly be suitable to monitor dynamic phenomena on the earth and repetitive observation is required irrelevant of "optical visibility" circumstance [13]. For this reason, SAR images derived from interferometric, polarimetric, or tomographic acquisitions have been widely employed to extract the forest parameters including canopy height [14]–[16], stem volume [17], and above-ground biomass [18]–[21] by given digital elevation models. In spite of that, they are still unable to measure the vertical structure under the canopy surface. An airborne profiling radar system named as HUTSCAT with *X*-band and *C*-band was designed to resolve such penetration problems, and detected a reflected signal from the ground surface and above-ground vegetation structures in 1990s [22], [23]. A more light-weighted *Ku*-band frequency-modulated continuous waveform (FMCW) profiling radar, called Tomoradar, was designed by the Finnish Geospatial Research Institute to collect the full polarization backscattered signals from forest in Finland on an airborne platform [24]–[26]. In this paper, the estimation of canopy height is investigated on the basis of Tomoradar waveform data.

In this work, an algorithm to estimate canopy height in a half-managed boreal forest from the Tomoradar waveform data are developed by, first, filtering noise with a weighted filtering method based on statistical properties of noise and, second, extracting location of the canopy top and ground based on a threshold of three times standard deviation of noise and last local maximum point. Meantime, the higher-precision reference data from the point cloud collected by a Velodyne VLP-16 laser scanner and the existing digital terrain model (DTM) are introduced to validate the accuracy of extracted canopy height. In this paper, we intend to investigate the feasibility of using profile radar as single sensor to derive canopy height with the proposed processing algorithm and evaluate its accuracy for potential applications in forestry.

The rest of this paper is organized as follows. Section II describes the Tomoradar system, its collected waveforms and reference data from LiDAR and DTM. Section III illustrates the algorithm of waveform processing and referenced canopy height resolving. Section IV expounds the results of canopy heights including mean error, root-mean-square error (RMSE), and correlation coefficient. Finally, the conclusions are given in Section V.

II. Dataset

The Tomoradar system collected data using a Bell 206 helicopter as the platform, which flew at 60–100 meters altitude with a flight velocity of 10–20 m/s. The Tomoradar was mounted on an extended arm of the helicopter and observed the nadir direction with an aluminum frame. Meanwhile, a Novatel tightly coupled GNSS-IMU system attached on the frame offered high-precision trajectory information of the helicopter with centimeter-level accuracy. The field test was carried out on 21st September, 2016 in an area located in southern Finland (61°19′N, 25°11′E) which was a part of the southern Boreal Forest Zone and consisted of predominantly of Scots pine, Norway spruce, and birch. The test site was divided into three parts: East, West, and South part, and the experimental data in this paper were collected in the West part, which is shown in Fig. 1.

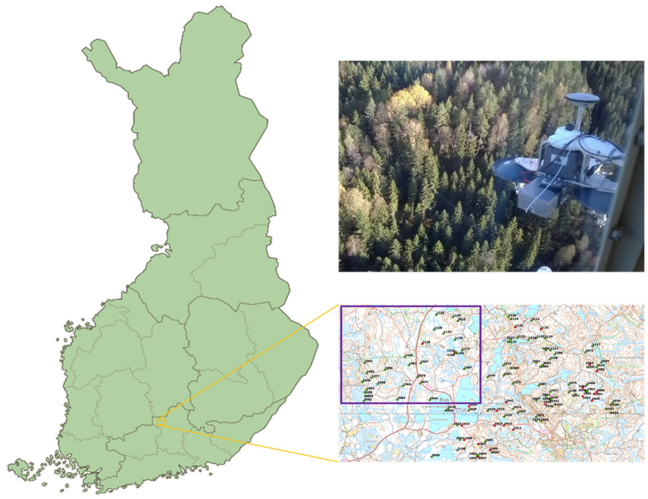

Fig. 1. Map of test site and its location in Finland. The purple box overlay on the site map indicates the west part where the waveform was collected, and the upper-right subfigure presents the Tomoradar in the field test.

Tomoradar transmits a *Ku*-band modulated (center frequency 14 GHz with 1 GHz sweep frequency) microwave radiation with a divergence of 6° (3 dB) into forest and receives the backscattered signals reflected from the surface of forest canopy and the ground. The received signals are converted into waveforms and recorded by a digitizer with 2.5 M/s sampling rate, all of which are processed in a postprocessing way. The Tomoradar receiver is capable of receiving signals in four polarization modes (VV, VH, HV, and HH) with 163 Hz modulation frequency. The 32 stripes of HH-polarization mode radar data (each contains 10 002 measurements) are utilized to explore the method of estimating the canopy height. The raw profile description of one stripe is shown in Fig. 2(a). The signal strength of the backscatter is illustrated by the right color bar of the figure, and the amplitude of the backscatter is proportional to the reflection cross section (RCS) observed from canopy top to the ground. A single backscatter profile measurement at the orange line marked location in this stripe is illustrated in Fig. 2(b).

Through Fig. 2, the single waveform can be regarded as a distance-resolved measure of microwave radiation backscattered from the canopy surface to the underlying ground.

Apart from the data mentioned above, dense airborne LiDAR point cloud data collected by a Velodyne VLP-16 laser scanner installed on the same platform of the helicopter and the DTM data of the test region generated by other means are also available, which are directly utilized as reference data to evaluate the experiment results. The precision of these data approaches

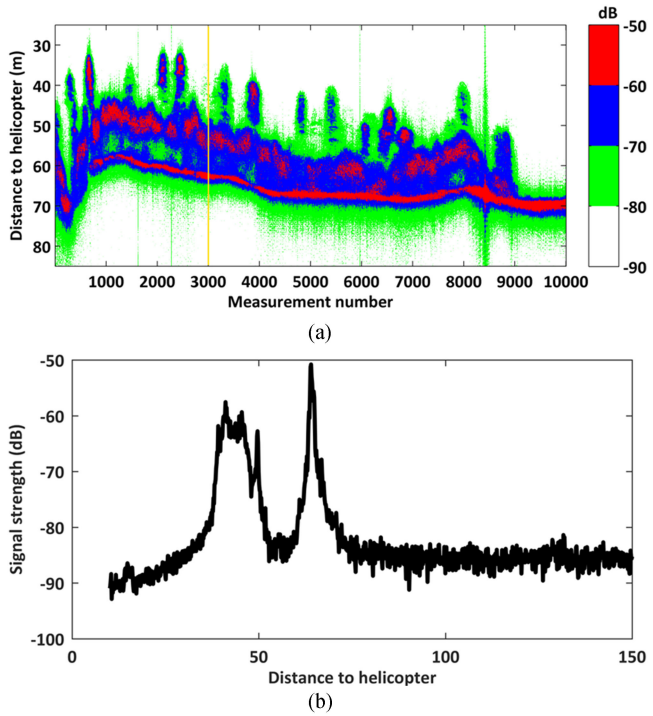

Fig. 2. (a) Raw Tomoradar waveform profiles in one stripe of HH mode. (b) Single waveform profile of one measurement at the orange marked location.

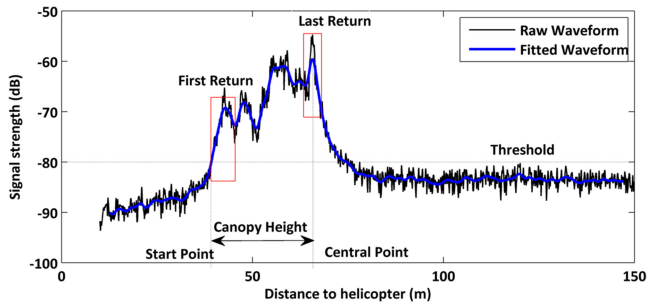

Fig. 3. Illustration of Tomoradar waveform and the derived canopy height.

approximately to several centimeter level. Thus, it is accurate enough to be selected as a reference to validate our algorithm.

III. Methodology

The Tomoradar waveforms are the records of the amplitude of backscattered microwave energy reflected from the target's surface as a function of distance. The concept of waveform is illustrated in Fig. 3, which gives an interpretation for measuring the vertical distribution of vegetation within the Tomoradar footprint. Based on the principle of FMCW radar, the starting point above the threshold is treated as the location of the canopy top and the last local maximum point is used to determine the range to the ground, and the subtraction of the canopy top and the ground should be the estimated canopy height.

The accuracy of estimating canopy height would descend with the reduction of the signal-to-noise ratio. To tackle this problem, we develop an algorithm similar to LiDAR full-waveform

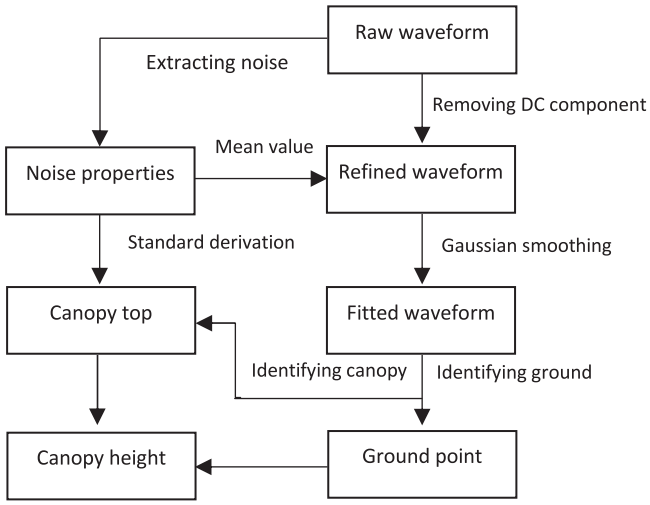

Fig. 4. Flowchart of deriving canopy height from Tomoradar waveform.

processing method, in order to mitigate noise with a weighted filter based on statistical properties of noise and identify ground point and canopy top to extract canopy height. The processing steps of the canopy height extraction from Tomoradar waveform is briefly shown in Fig. 4.

Considering that the length of the recorded Tomoradar waveform is usually longer than the maximum target range, the mean value and standard deviation of noise can be calculated on the basis of the latter part of the waveform, for example, from 100 to 150 m in Fig. 3. We regard the mean value of the noise as a dc component and subtract it from the raw waveform to obtain the refined waveform. Thus, the refined waveform can be expressed

$$P_s(d) = P_r(d) - M_n \tag{1}$$

where $P_r(d)$ and $P_s(d)$ are the raw waveform and the converted waveform, respectively, and M_n is the mean value of the noise.

Then, the noise level of the backscattered signals can be substantially decreased by adopting a weighted averaging method. According to the character of the waveform, we select a normalized Gaussian function as a filter and describe it by [27]

$$f(d) = \frac{1}{\sqrt{2\pi}\omega} \exp\left(-\frac{d^2}{2\omega^2}\right). \tag{2}$$

Here, ω is the root mean square width of the Gaussian function, the value of which is determined by the width of the received waveform from the flat ground, the same way the LiDAR waveform is processed [28].

The Gaussian smoothing is applied to filter noise by convolving the refined waveform with the Gaussian weight. To greatly reduce the noise effects and obtain superior fitted waveform, the convolution window is set to contain 30 signals in this paper.

Next, we employ a local maximum based on the zero-crossing algorithm [29] to extract the local maximum points (LMP) of the fitted waveform. Only the amplitudes of the fitted waveform at the extracted LMPs that are larger than a certain threshold (three times standard derivation of the noise) are preserved to determine the canopy top and ground. These are called effective LMPs.

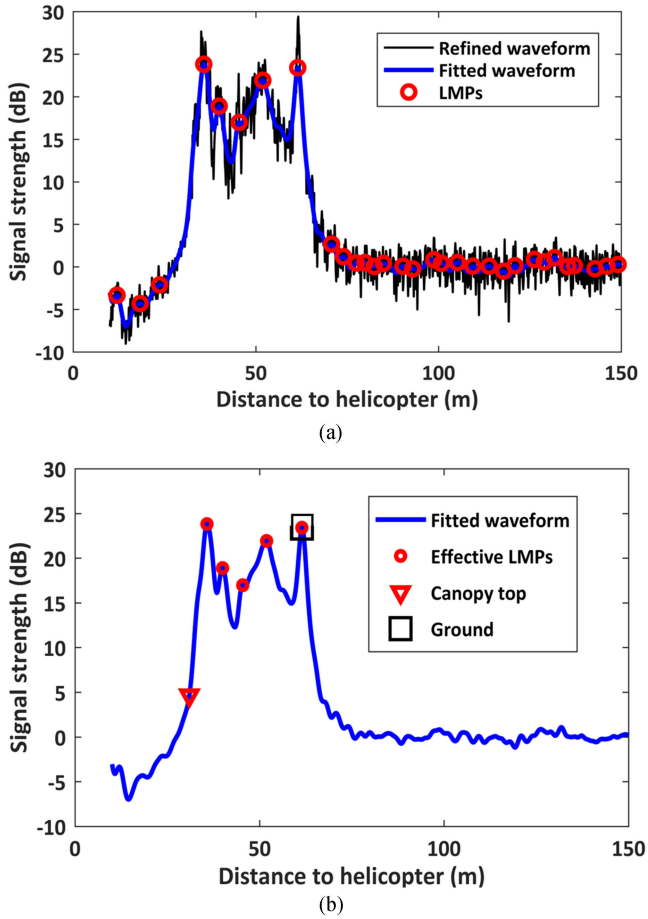

Fig. 5. Illustration of Tomoradar waveform processing. (a) Gaussian smoothing and extracted LMPs. (b) Effective LMPs and identified canopy top and ground.

The canopy top is identified as the first location d_c prior to the first effective LMP within the fitted waveform above the threshold [30], [31]. We then acquire the center of the ground return (approximately the centroid of Tomoradar footprint on the ground) d_g by searching for the last one of the effective LMPs of the fitted waveform. Fig. 5 demonstrates an example of determining LMPs, the canopy top and ground.

As shown in Fig. 5, Gaussian smoothing is dramatically beneficial to diminish the influence of noise on Tomoradar waveform. The LMPs and effective LMPs can be recognized from the fitted waveform based on zero-crossing algorithm and the threshold. Then, we directly extract canopy top and ground level according to their identification ways.

Consequently, the canopy height can be calculated by the two locations as

$$h = d_g - d_c. \tag{3}$$

To reasonably verify the accuracy of canopy height, we only use the LiDAR cloud point and DTM data when pitch and roll angle of the helicopter are approximately close to zero. Due to the zigzag flight trajectory, approximately 40% original data are selected to be investigated. The principle of determining the canopy height based on the reference data are shown in Fig. 6.

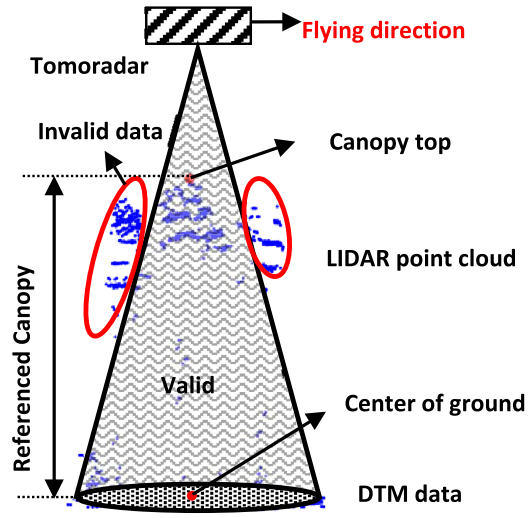

Fig. 6. Estimation of canopy height using reference data.

The reference data merely restricted inside the cone, which is generated by the Tomoradar microwave radiation with divergence angle of six degrees, are valid to calculate the referenced canopy height. Among these valid data, the peak point derived from LiDAR point cloud data which are closest to the helicopter can be considered as the canopy top, and the distance of center of ground to the helicopter is expressed roughly by the difference between the height of helicopter the mean height of DTM data within Tomoradar footprint. Finally, we obtain reference value of canopy height by calculating the range from the peak point of LiDAR point cloud to the central point of the Tomoradar footprint on the ground.

IV. Result and Discussion

We first apply the proposed algorithm to the previously mentioned Tomoradar waveforms dataset. The processed results of two waveforms originated from the fourth stripe with different penetration into vegetation are shown in Fig. 7, which demonstrates that the algorithm can effectively distinguish the actual signal and noise.

The proposed algorithm can provide accurate position of canopy top and ground for most Tomoradar waveforms, except for a few waveforms with only single-peak signal when microwave radiation is incident directly on the ground surface. Therefore, we just employ the waveforms composed of both vegetation returns and ground returns, and abandon other inappropriate waveforms in this paper.

To quantitatively validate the accuracy of the waveform processing algorithm, we compare the canopy top and the ground extracted from the waveforms with the coincident results calculated from reference data, which can be considered as the ground truth. Hence, we describe the error distributions of canopy top and ground versus measurement numbers of fourth stripe in Fig. 8, only 2336 measurements of which remain when the conditions of the nadir observation of Tomoradar and multiple targets contained in the backscatter waveform conform to the rules in this paper.

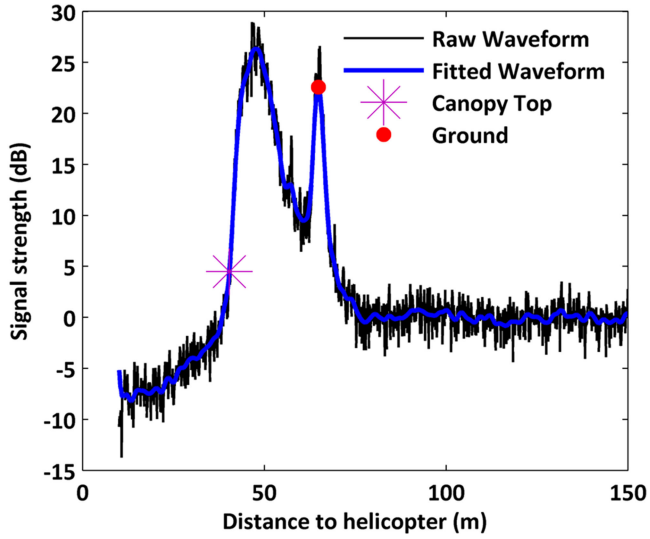

(a)

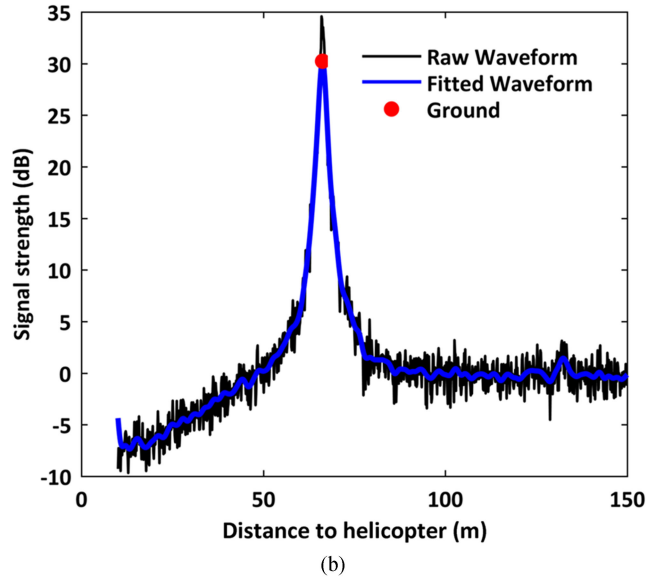

(b)

Fig. 7. Processed waveforms from two typical targets. (a) Mixture of vegetation and ground. (b) Only ground. The mean of noise is adjusted to be zero for all processed waveforms.

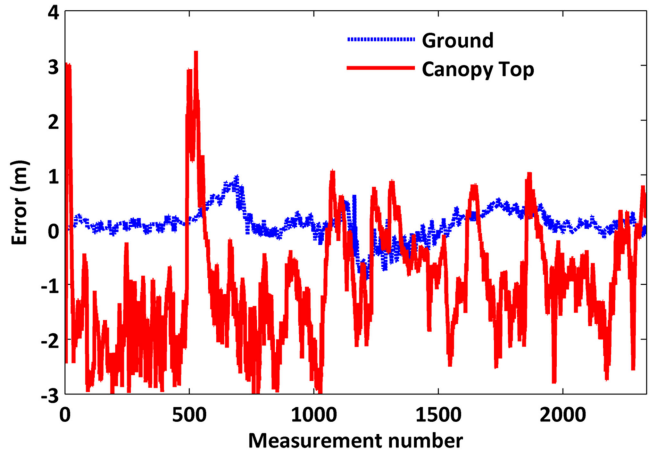

Fig. 8. Error distributions of canopy top and ground resolved from the Tomoradar waveforms.

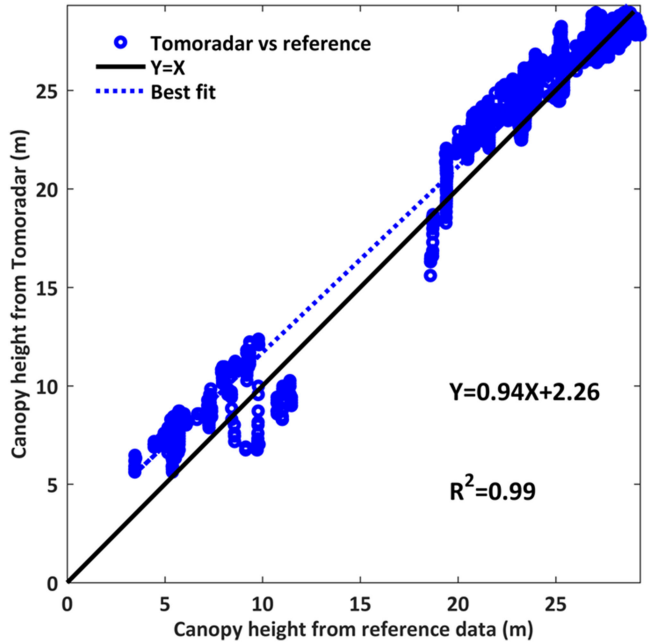

Fig. 9. Comparison of canopy height within footprint between HH mode Tomoradar and reference data from the 5th stripes measurements.

The error of canopy top is obviously greater than that of ground in Fig. 8, and the reason is that the configuration of vegetation is much more complicated than morphology of ground. Many factors related to vegetation structure, including the composition, geometry, roughness, and density of canopy components within the Tomoradar footprint, have a strong effect on determining the distance of canopy top. The results show that the RMSE is 1.07 m for the canopy top and 0.27 m for the ground, and mean error is −1.01 m for the canopy top estimation and 0.1 m for the ground estimation. It can be observed that the canopy top measurement of Tomoradar is generally a little bit lower than that from LiDAR. The explanation is straightforward, that the minimum RCS of Tomoradar is larger than that of LiDAR. It does not imply that Tomoradar is less sensitive, but just explain the physical phenomenon that only when the backscattered energy reflected by the canopy top in 6° divergence of Tomoradar is higher than the background noise, the waveform of canopy top can be observed in microwave radar measurement. However, the divergence of LiDAR is normally in milliradian level; for boreal coniferous forest, it is common that LiDAR can detect the top of coniferous tree, such as pine and spruce, within its much smaller footprint (normally several centimeters diameter), while microwave radar cannot observe such small flat facet within its several meters diameter footprint. Thus, Tomoradar needs larger RCS; due to the cone shape of the tree canopy of coniferous tree and nadir observation condition, the detected canopy top should be lower than LiDAR measurement. From Fig. 8, we can also observe that there are

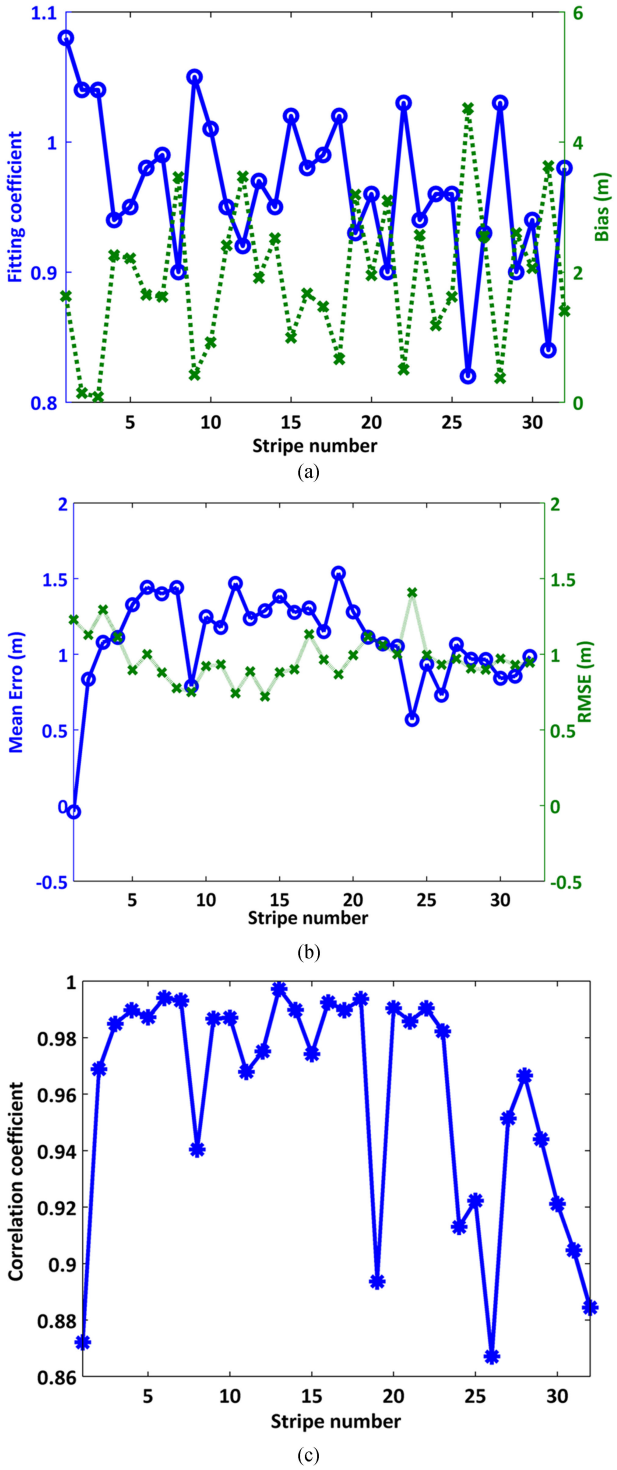

Fig. 10. Extracted canopy height results analysis for different stripe numbers. (a) Comparison between Tomoradar and reference data sequenced by the stripe order of left-to-right and up-to down. (b) Mean error and RMSE. (c) Correlation coefficient.

some Tomoradar canopy top measurements higher than that of LiDAR, and the reason is the side lobes of the antenna pattern. The antenna pattern is usually strongly peaked along the beam axis, and the spatial resolution is defined by the angular region over which the antenna power pattern is less than 3 dB down from its value at beam center. However, all antennas have side lobes and some of the received energy comes from the outside of the main 3 dB area. Thus, this can lead to some ambiguities due to radiation collected via the side lobes and misinterpreted as radiation in the main lobe [8].

Using the exported results of the canopy top and ground from the waveforms with the proposed processing method, we compute the distributions of the canopy height and compare them to the actual canopy height determined by reference data. We present a scatterplot of canopy height from Tomoradar data versus canopy height from reference data in Fig. 9 with linear fit.

When comparing canopy height obtained from Tomoradar waveforms and reference data for 2336 measurements, the derived Tomoradar canopy heights correlate well to those from reference data with a higher correlation coefficient ($R^2 = 0.99$) and a mean error of 1.11 m and RMSE of 1.12 m. The fitting coefficient and bias are 0.94 and 2.26 m, respectively. The linear regression model produces an excellent goodness of fit with the coefficient of determination of 96%.

As an ultimate validation of the approach of canopy height using Tomoradar waveforms, the estimated results were compared with those of reference data for a total of 32 stripes. The fitting coefficients, biases, mean errors, RMSE, and correlation coefficients of the canopy height for different stripes are shown in Fig. 10, in which all useful data volume approaches to 127 765 measurements.

In total, 127 765 copolarization measurements from 32 stripes of the Tomoradar field test were processed by the proposed fitting algorithm to mitigate the measurement noise, and the canopy height results were compared with those from reference data. The mean error of canopy height changed from -0.04 to 1.53 m, and the RMSE approached to 1 m. Since the RMSE of the ground maintains at several decimeters level (0.3 m), the RMSE of canopy height is majorly contributed by the estimation uncertainty of canopy top measurement. Through Fig. 9, the canopy height from one stripe of Tomoradar data versus that from reference data converge around the straight line of $Y = X$ (fitting coefficients vary from 0.82 to 1.08 for all 32 stripes), and the corresponding biases have a wide range from 0.08 to 4.52 m. The linear regression models also produce great goodness of fit with the coefficient of determination ranging from 75% to 99%. Meanwhile, the correlation coefficients of the selected data varying from 0.86 to 0.99 demonstrate that the extracted canopy height correlates highly with the referenced results, and the average value of the correlation coefficients for the selected data are close to 0.96.

V. Conclusion

In this work, an algorithm has been proposed to estimate canopy height from Tomoradar copolarization waveforms. After filtering waveforms based on the statistical properties of noise, the position of canopy top and ground can be obtained according to the threshold and noise level. The canopy height can be subsequently calculated by the difference between canopy top and ground position. To validate the accuracy of extracted

canopy height, we utilize centimeter-level reference data including DTM data and LiDAR point cloud from Velodyne VLP-16.

The results of this paper indicate that Tomoradar can be applied in the accurate measurement of canopy height with approximately 1 m accuracy and its correlation to the references data are above 0.9. It has been demonstrated that Tomoradar provides a new pattern in estimation of canopy height using a larger footprint, and is capable of becoming a validation instrument for satellite LiDAR in the forest inventory. Our future work is to improve the RMSE of estimation results by using a more appropriate set of thresholds such as the vegetation type and growth age. Other types of forest will also be investigated to verify its generic applicability.

REFERENCES

[1] A. T. Hudak, M. A. Lefsky, W. B. Cohen, and M. Berterretche, "Integration of LiDAR and Landsat ETM+ data for estimating and mapping forest canopy height," *Remote Sens. Environ.*, vol. 82, no. 2/3, pp. 397–416, 2002.

[2] D. O. Mcinerney, J. Suarez-Minguez, R. Valbuena, and M. Nieuwenhuis, "Forest canopy height retrieval using LiDAR data, medium-resolution satellite imagery and *k*NN estimation in Aberfoyle, Scotland," *Forestry*, vol. 83, no. 2, pp. 195–206, 2010.

[3] A. Khosravipour, A. K. Skidmore, M. Isenburg, T. Wang, and Y. A. Hussin, "Generating pit-free canopy height models from airborne LiDAR," *Photogrammetric Eng. Remote Sens.*, vol. 80, no. 9, pp. 863–872, 2014.

[4] M. Wang, R. Sun, and Z. Xiao, "Estimation of forest canopy height and aboveground biomass from spaceborne LiDAR and Landsat imageries in Maryland," *Remote Sens*., vol. 10, no. 2, p. 344, 2018, [Online]. Available: http://www.mdpi.com/2072-4292/10/2/344

[5] M. García, S. Saatchi, S. Ustin, and H. Balzter, "Modelling forest canopy height by integrating airborne LiDAR samples with satellite radar and multispectral imagery," *Int. J. Appl. Earth Observ. Geoinformation*, vol. 66, pp. 159–173, 2018.

[6] P. Gong, X. Mei, G. S. Biging, and Z. Zhang, "Improvement of an oak canopy model extracted from digital photogrammetry," *Photogrammetric Eng. Remote Sens.*, vol. 63, no. 9, pp. 919–924, 2002.

[7] Y. Sheng, P. Gong, and G. S. Biging, "Model-based conifer canopy surface reconstruction form photographic imagery: Overcoming the occlusion, foreshortening, and edge effects," *Photogrammetric Eng. Remote Sens.*, vol. 69, no. 3, pp. 249–258, 2003.

[8] C. Song and M. B. Dickinson, "Extracting forest canopy structure from spatial information of high resolution optical imagery: Tree crown size versus leaf area index," *Int. J. Remote Sens.*, vol. 29, no. 19, pp. 5605–5622, 2008.

[9] M. Alonzo, B. Bookhagen, J. P. McFadden, A. Sun, and D. A. Roberts, "Mapping urban forest leaf area index with airborne LiDAR using penetration metrics and allometry," *Remote Sens. Environ.*, vol. 162, pp. 141–153, 2015.

[10] L. Chen, T. Chiang, and T. Teo, "Fusion of LiDAR data and high resolution images for forest canopy modeling," in *Proc. 26th Asian Conf. Remote Sens.*, 2005.

[11] J. Zhou *et al.*, "Tree crown detection in high resolution optical and LiDAR images of tropical forest," in *Proc. Remote Sens. Agriculture, Ecosystems, Hydrology XII*, SPIE, vol. 7824, 2010.

[12] J. A. Jackson and R. L. Moses, "Clutter model for VHF SAR imagery, Algorithms for synthetic aperture radar imagery XI," *Int. Soc. Opt. Photon.*, vol. 5427, pp. 271–283, 2004.

[13] C. Elachi and J. J. Van Zyl, *Introduction to the Physics and Techniques of Remote Sensing*. New York, NY, USA: Wiley, 2006.

[14] H. Balzter, A. Luckman, L. Skinner, C. Rowland, and T. Dawson, "Observations of forest stand top height and mean height from interferometric SAR and LiDAR over a conifer plantation at Thetford Forest, UK," *Int. J. Remote Sens.*, vol. 28, no. 6, pp. 1173–1197, 2007.

[15] J. Praks, C. Demirpolat, O. Antropov, and M. Hallikainen, "On forest height retrieval from spaceborne X-band interferometric SAR images under variable seasonal conditions," in *Proc. XXXIII Finnish URSI Conv. Radio Sci. SMARAD Seminar*, Otaniemi, Finland, 2013, vol. 2425, pp. 115–118.

[16] S. Kumar, S. K. Joshi, and H. Govil, "Spaceborne PolSAR tomography for forest height retrieval," *IEEE J. Sel. Topics Appl. Earth Observ. Remote Sens.*, vol. 10, no. 12, pp. 5175–5185, Dec. 2017.

[17] M. Santoro, J. Askne, G. Smith, and J. E. Fransson, "Stem volume retrieval in boreal forests from ERS-1/2 interferometry," *Remote Sens. Environ.*, vol. 81, no. 1, pp. 19–35, 2002.

[18] M. Neumann, S. S. Saatchi, L. M. Ulander, and J. E. Fransson, "Assessing performance of L-and P-band polarimetric interferometric SAR data in estimating boreal forest above-ground biomass," *IEEE Trans. Geosci. Remote Sens.*, vol. 50, no. 3, pp. 714–726, Mar. 2012.

[19] R. Treuhaft *et al.*, "Tropical-forest biomass estimation at X-band from the spaceborne TanDEM-X interferometer," *IEEE Geosci. Remote Sens. Lett.*, vol. 12, no. 2, pp. 239–243, Feb. 2015.

[20] D. H. T. Minh, T. Le Toan, F. Rocca, S. Tebaldini, M. M. d'Alessandro, and L. Villard, "Relating P-band synthetic aperture radar tomography to tropical forest biomass," *IEEE Trans. Geosci. Remote Sens.*, vol. 52, no. 2, pp. 967–979, Feb. 2014.

[21] D. H. T. Minh, S. Tebaldini, F. Rocca, T. Le Toan, L. Villard, and P. C. Dubois-Fernandez, "Capabilities of BIOMASS tomography for investigating tropical forests," *IEEE Trans. Geosci. Remote Sens.*, vol. 53, no. 2, pp. 965–975, Feb. 2015.

[22] M. Hallikainen *et al.*, "A helicopter-borne eight-channel ranging scatterometer for remote sensing. I. System description," *IEEE Trans. Geosci. Remote Sens.*, vol. 31, no. 1, pp. 161–169, Jan. 1993.

[23] J. Hyyppa and M. Hallikainen, "A helicopter-borne eight-channel ranging scatterometer for remote sensing. II. Forest inventory," *IEEE Trans. Geosci. Remote Sens.*, vol. 31, no. 1, pp. 170–179, Jan. 1993.

[24] L. Piermattei *et al.*, "Comparing helicopter-borne profiling radar with airborne laser scanner data for forest structure estimation," in *Proc. EGU General Assem. Conf. Abstr.*, 2017, vol. 19, p. 13741.

[25] Y. Chen *et al.*, "UAV-borne profiling radar for forest research," *Remote Sens*., vol. 9, no. 1, p. 13741, 2017.

[26] Z. Feng, Y. Chen, T. Hakala, and J. Hyyppä, "Range calibration of airborne profiling radar used in forest inventory," in *Proc. IEEE Int. Geosci. Remote Sens. Symp.*, 2016. pp. 6672–6675, [Online]. Available: http://www.mdpi.com/2072-4292/9/1/58

[27] C. E. Parrish, I. Jeong, R. D. Nowak, and R. B. Smith, "Empirical comparison of full-waveform LiDAR algorithms," *Photogrammetric Eng. Remote Sens.*, vol. 77, no. 8, pp. 825–838, 2011.

[28] M. A. Hofton, J. B. Minster, and J. B. Blair, "Decomposition of laser altimeter waveforms," *IEEE Trans. Geosci. Remote Sens.*, vol. 38, no. 4, pp. 1989–1996, Jul. 2000.

[29] W. Wagner, A. Ullrich, V. Ducic, T. Melzer, and N. Studnicka, "Gaussian decomposition and calibration of a novel small-footprint full-waveform digitising airborne laser scanner," *ISPRS J. Photogrammetry Remote Sens.*, vol. 60, no. 2, pp. 100–112, 2006.

[30] D. J. Harding, M. A. Lefsky, G. G. Parker, and J. B. Blair, "Laser altimeter canopy height profiles: Methods and validation for closed-canopy, broadleaf forests," *Remote Sens. Environ.*, vol. 76, no. 3, pp. 283–297, 2001.

[31] M. A. Lefsky, M. Keller, Y. Pang, P. B. De Camargo, and M. O. Hunter, "Revised method for forest canopy height estimation from Geoscience Laser Altimeter System waveforms," *J. Appl. Remote Sens.*, vol. 1, no. 1, 2007, Art. no. 013537.

Hui Zhou received the B.S. and M.S. degrees in mechanical design and optical engineering and the Ph.D. degree in geodesy and survey engineering from Wuhan University, Wuhan, China, in 2001, 2003, and 2007, respectively. His dissertation focused on the theoretical modeling and data processing with geoscience laser altimeter system onboard the ICESat.

He is currently an Associate Professor with Wuhan University, where he is involved with the development of laser retroreflector arrays on satellite and the application of space laser altimeter in land and vegetation. His research interests include theoretical modeling and data processing of spaceborne LiDAR, hyperspectral LiDAR, and radar technology.

Yuwei Chen received the B.E. and M.Sc. degree from Zhejiang University, Hangzhou, China, in 1999 and 2002, respectively, and the Ph.D. degree in circuits and systems from Shanghai Institute of Technical Physics (SITP), Chinese Academy of Science, Beijing, China, in 2005.

He is currently working with the Department of Remote Sensing and Photogrammetry, Finnish Geospatial Research Institute, Masala, Finland, as a research manager leading the research group Remote Sensing Electronics, which focuses on developing new remote sensing systems. He holds 10 patents and has authored and coauthored more than 120 scientific papers and book chapters. His research interests include spaceborne LiDAR, hyperspectral LiDAR, radar technology, and seamless navigation.

Juha Hyyppä received the M.Sc., Dr.Ing., and Dr.Sc. degrees (Hons.) from the Helsinki University of Technology, Espoo, Finland, in 1987, 1990, and 1994, respectively.

He is currently a Professor of remote sensing and photogrammetry and the Director of the Centre of Excellence in Laser Scanning Research, Finnish Geospatial Research Institute, Masala, Finland, and also a Distinguished Professor with Shinshu University, Matsumoto, Japan. He has 25 years of experience in research team leadership and in the coordination of more than ten international science projects. He has authored and coauthored more than 150 ISI Web of Science listed papers. His research interests include laser scanning systems, their performance and new applications, especially related to mobile, personal, and ubiquitous laser scanning, and their point cloud processing especially to forest information extraction.

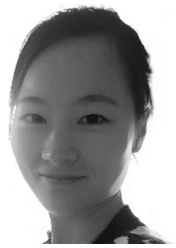

Ziyi Feng received the M.Sc. degree from the School of Electrical Engineering, Aalto University, Espoo, Finland, in 2016, where she is currently working toward the Ph.D. degree in space science.

She is currently a Research Scientist with the Finnish Geospatial Research Institute, Masala, Finland. Her research interests include microwave active and passive radar for forest investigation.

Fashuai Li received the B.S. degree in geodetic engineering and the M.S. degree in geographical information system from China University of Mining and Technology, Beijing, China, in 2011 and 2014, respectively. He is currently working toward the Ph.D. degree with the Department of Earth Observation Science at ITC, University of Twente, Enschede, The Netherlands.

He worked with the Beijing General Research Institute of Mining and Metallurgy in 2014. In 2017, he was a Research Visitor with the Finnish Geospatial Research Institute. His research interests include feature engineering, machine learning, radar technology, image and point cloud processing, especially the interpretation of urban objects in mobile laser scanning data.

Teemu Hakala is a Research Scientist with the Department of Remote Sensing and Photogrammetry, Finnish Geospatial Research Institute, Masala, Finland. His research interests include UAV sensor technology, radiometric measurements, hyperspectral environment monitoring, hyperspectral LiDAR, and radar technology.

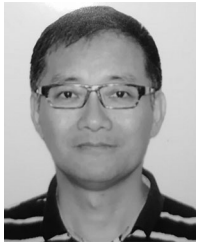

Xinmin Xu received the B.S., M.S., and Ph.D. degrees in electronics engineering from Zhejiang University, Hangzhou, China, in 1986, 1992, and 2007, respectively.

He is currently an Associate Professor of electronics engineering at Zhejiang University. He went to IMEC in Belgium to join a training program in semiconductor technology in 2006. He participates in national high-tech projects, and the National Natural Science Fund as Co-PIs, and hosts several projects funded by Zhejiang Provincial Science and Technology Bureau. He holds 14 authorized patents and has authored and coauthored more than 50 scientific papers including ISI Web of Science listed papers and several book chapters.

Xiaolei Zhu received the B.S. and M.S. degrees in electrical engineering from Zhejiang University, China, in 2000 and 2003, respectively. He received the Ph.D. degree in electronic engineering from Keio University, Tokyo, Japan, in 2012.

From 2003 to 2006, he was with the Institute of Micro-electronics, Tsinghua University, Beijing, China, as an Assistant Researcher. From 2007 to 2012, he was with Fujitsu Lab, Kawasaki, Japan, where he investigated high-performance A/D converters as a research intern. He has been an Assistant Professor with the Institute of VLSI Design, Zhejiang University, China, since 2012. His current research interests include the field of analog and mixed-signal integrated circuits and systems.